SAND2019-6636C

Polyhedral discretizations using tetrahedral subdivisions, aggregation, and optimization-based shape functions with applications to nonlinear solid mechanics

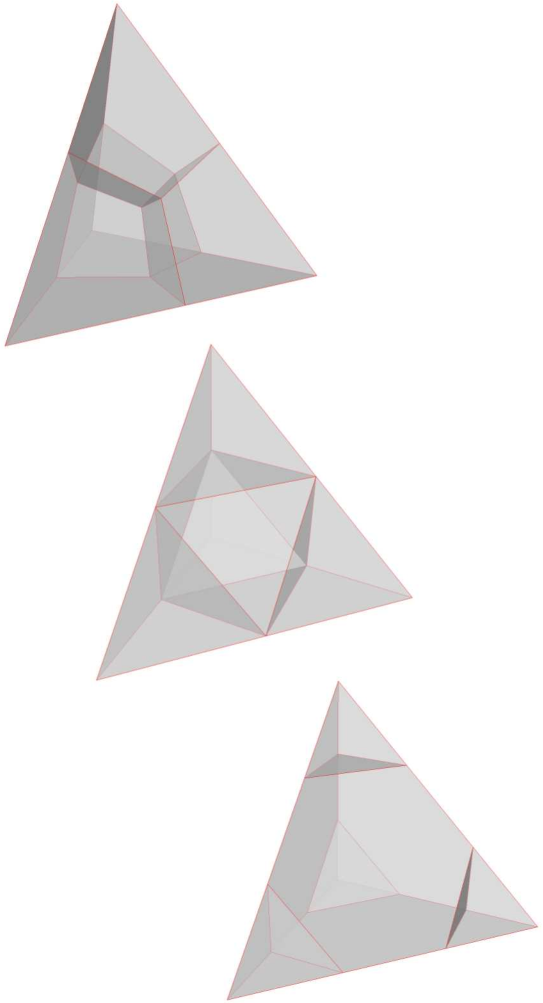

Joe Bishop
Engineering Sciences Center
Sandia National Laboratories
Albuquerque, NM

SIAM Conference on Computational Geometric Design
Vancouver, Canada, June 17-19, 2019

Sandia National Laboratories is a multimission laboratory managed and operated by National Technology and Engineering Solutions of Sandia, LLC, a wholly owned subsidiary of Honeywell International, Inc., for the U.S. Department of Energy's National Nuclear Security Administration under contract DE-NA-0003525.

Acknowledgement

Prof. Sukumar at UC Davis for active research discussions and use of his MAXENT library.

Bishop, J. and Sukumar, N., "Polyhedral finite elements for nonlinear solid mechanics using tetrahedral subdivisions and dual-cell aggregation," *Computer Aided Geometric Design*, (submitted)

Outline

1. motivation for polyhedral elements
2. tetrahedral subdivisions and polyhedral dual cells
3. governing equations for Lagrangian mechanics
4. finite element formulation (shape functions, quadrature)
5. examples (verification, nonlinear)

Why polyhedra?

- increased flexibility in finite element discretizations (tetrahedra and hexahedra are special cases)
- enables hybrid meshing, e.g. hexahedral-dominant using frame fields
- enables cut-cell approaches
- Voronoi meshing

cut-cell

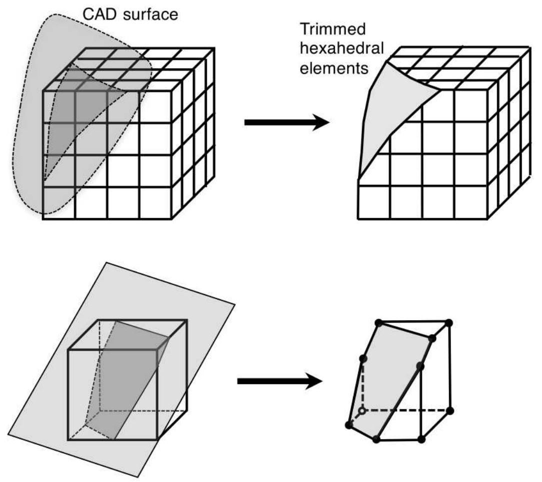

Kim, H.-G. and D. Sohn (2015). IJNME,**102,** 1527-1553.

Voronoi

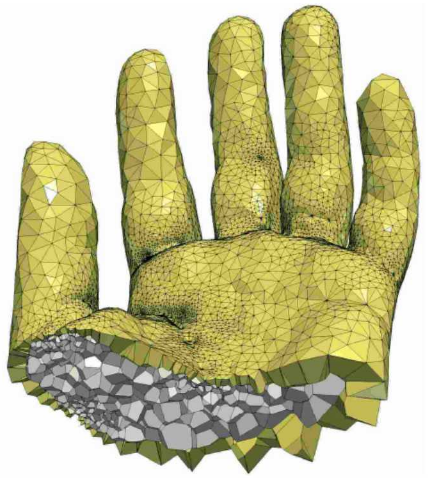

Abdelkader, A., et al. (2019). "VoroCrust: Voronoi meshing without clipping." arXiv preprint arXiv:1902.08767.

Another approach to forming polyhedral elements

Start with a tetrahedral mesh and then form dual polyhedral cells.

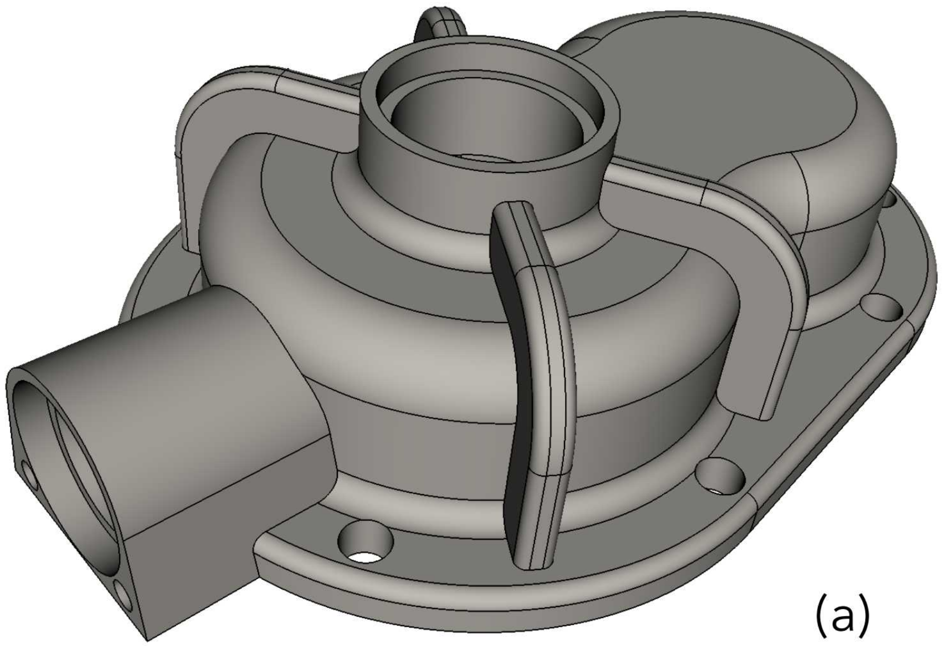

(a)

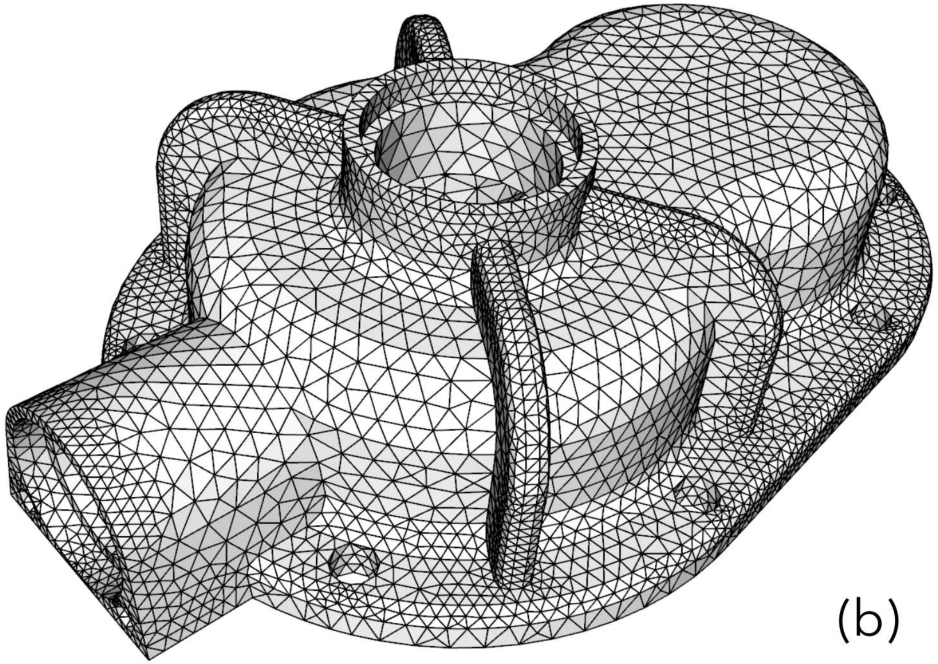

(b)

Three types of tetrahedral subdivision

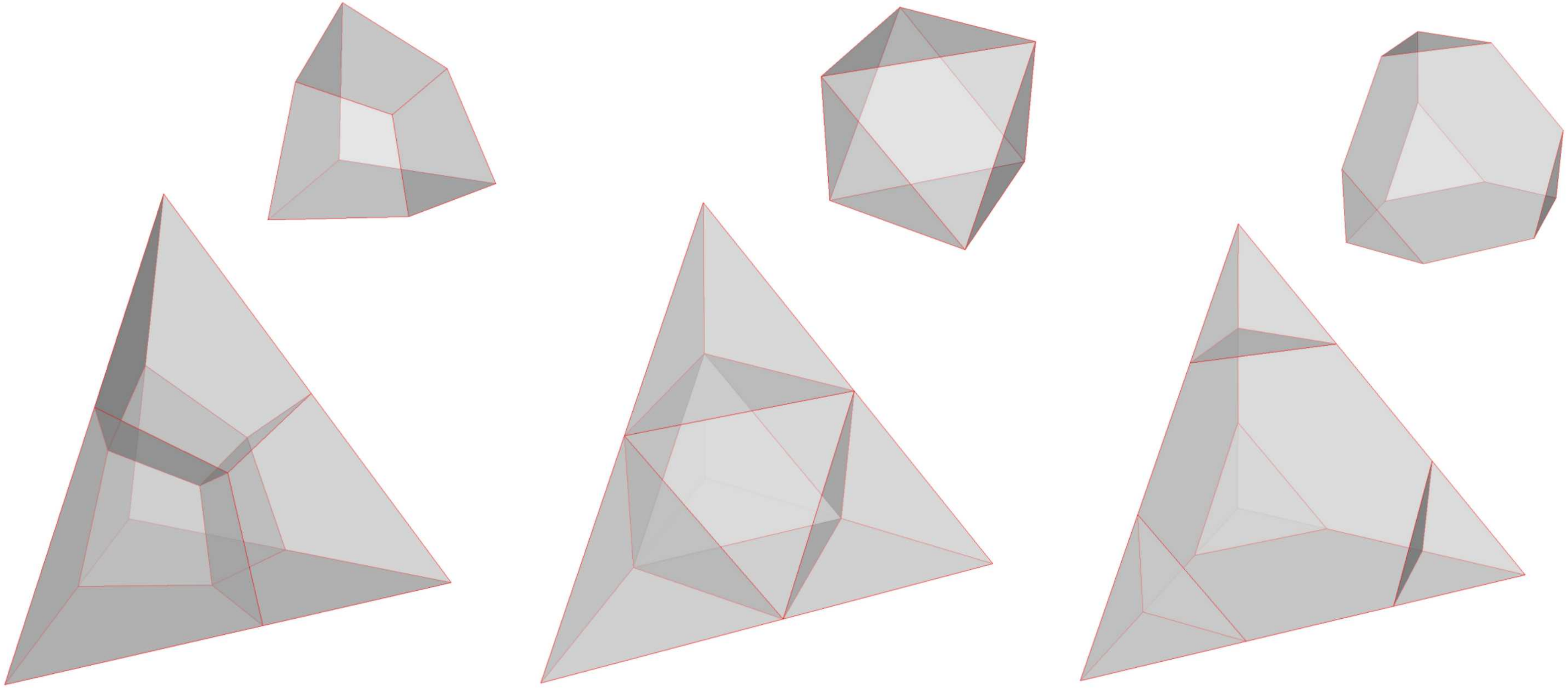

barycentric | full truncation | partial truncation

Barycentric subdivision and aggregation

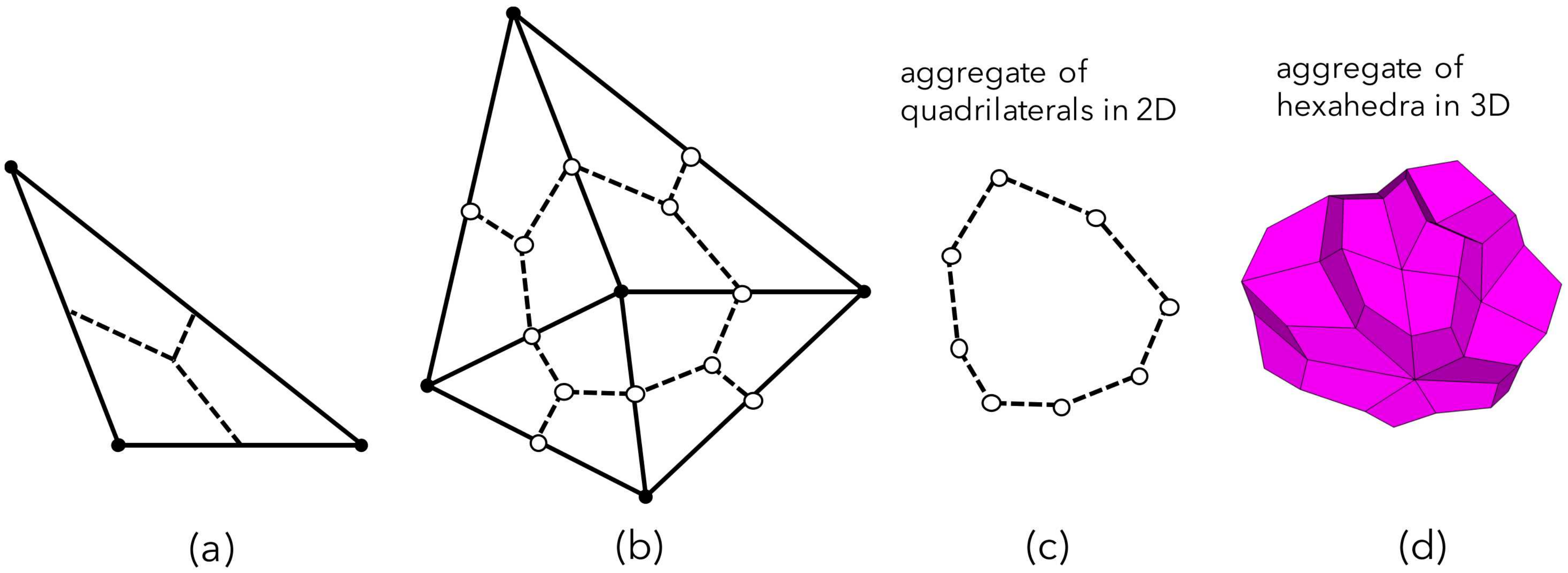

Barycentric subdivision and aggregation

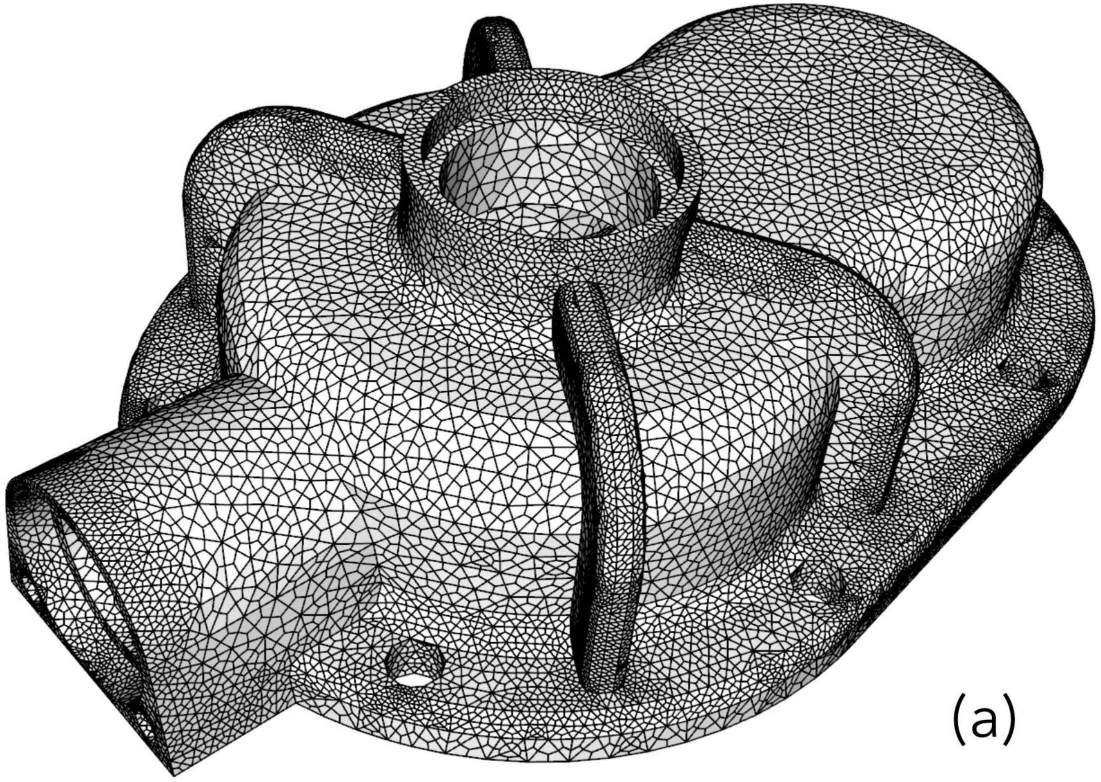

(a)

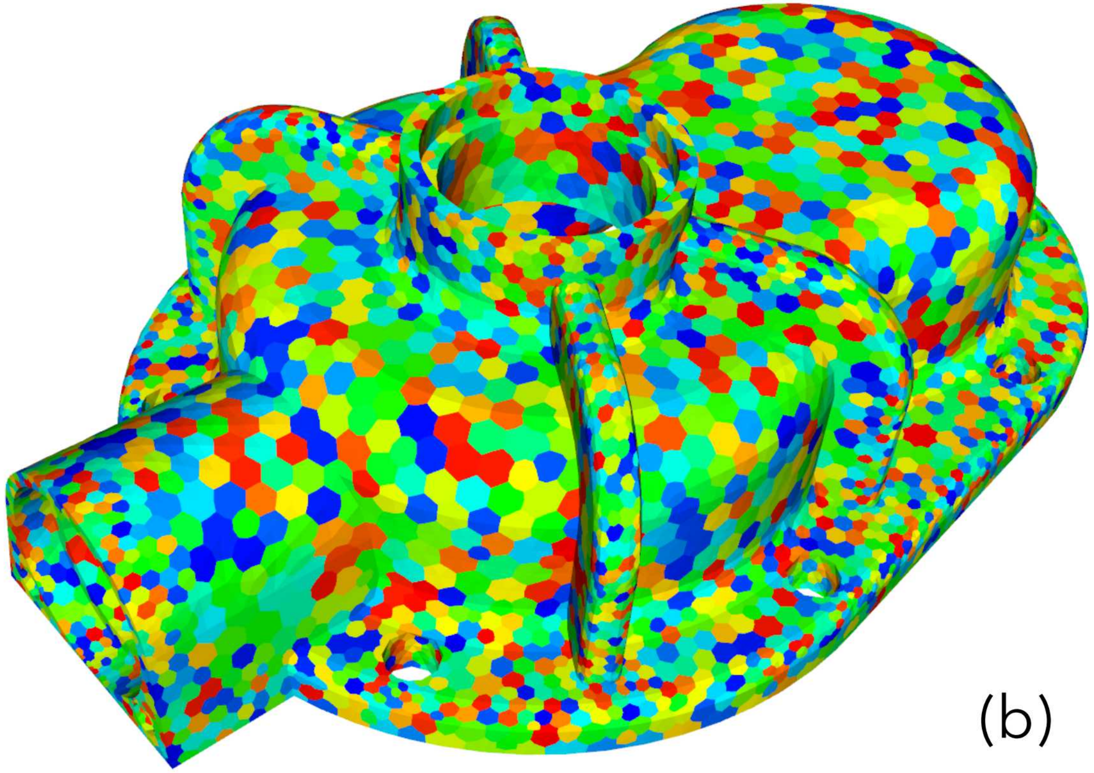

(b)

Full truncation and aggregation

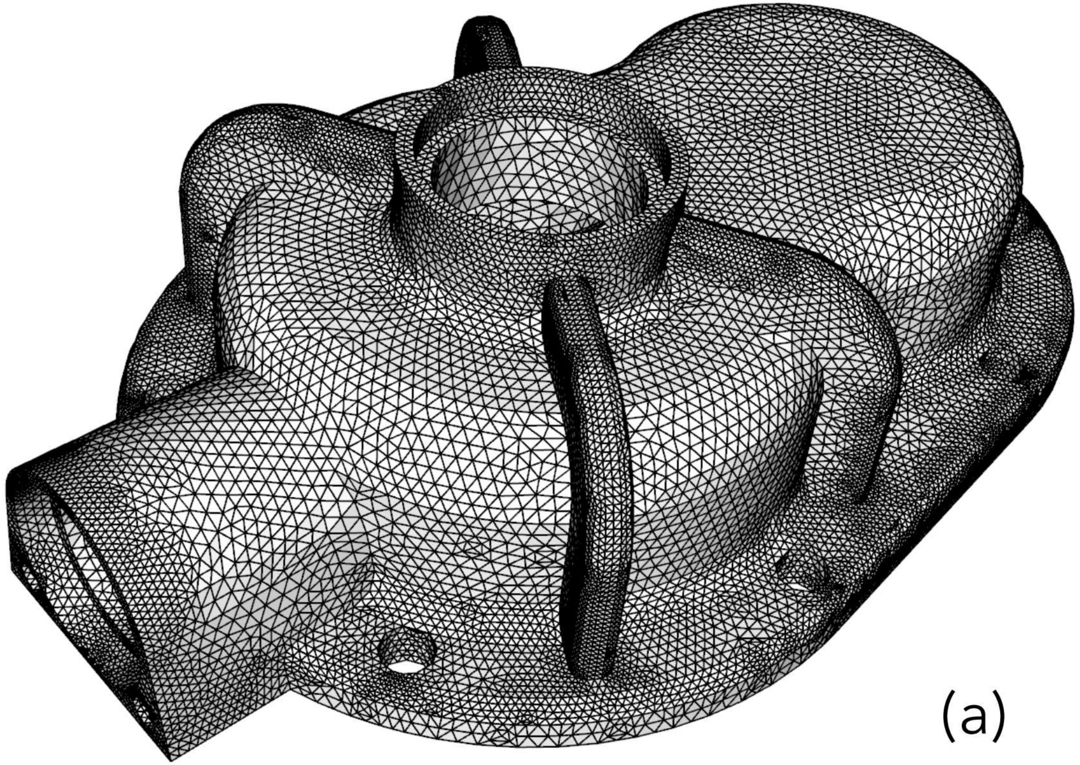

(a)

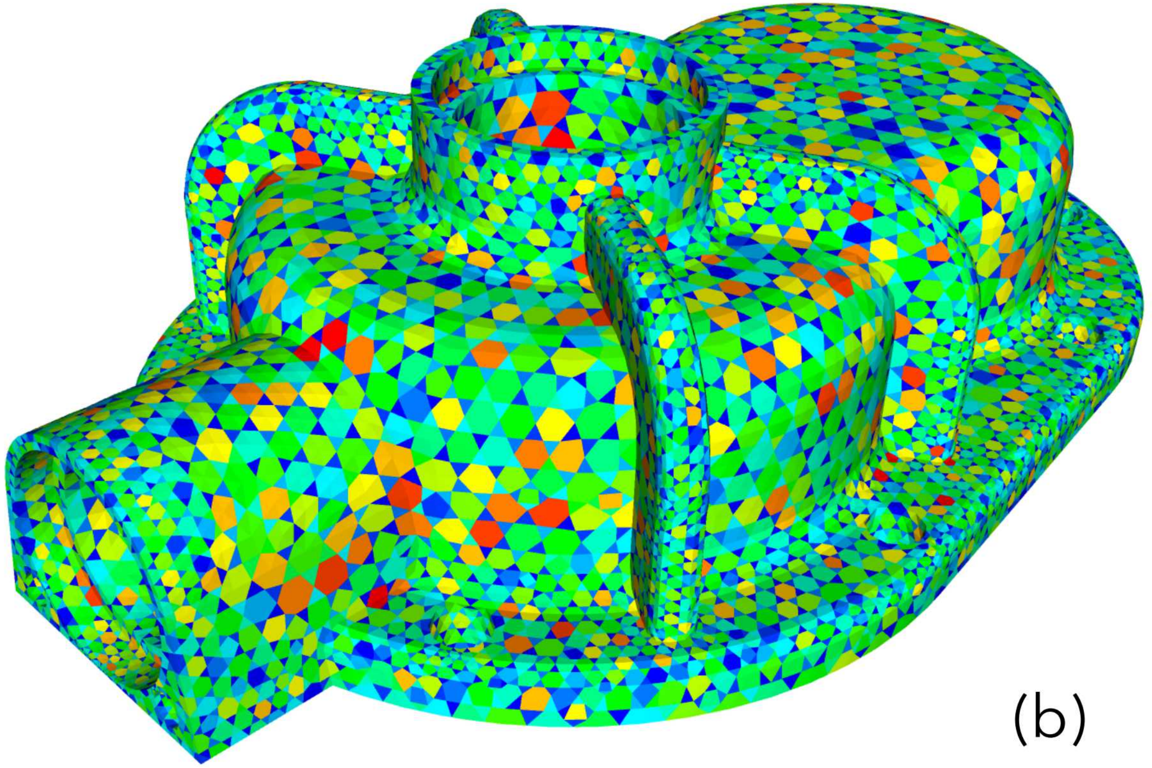

(b)

Partial truncation and aggregation

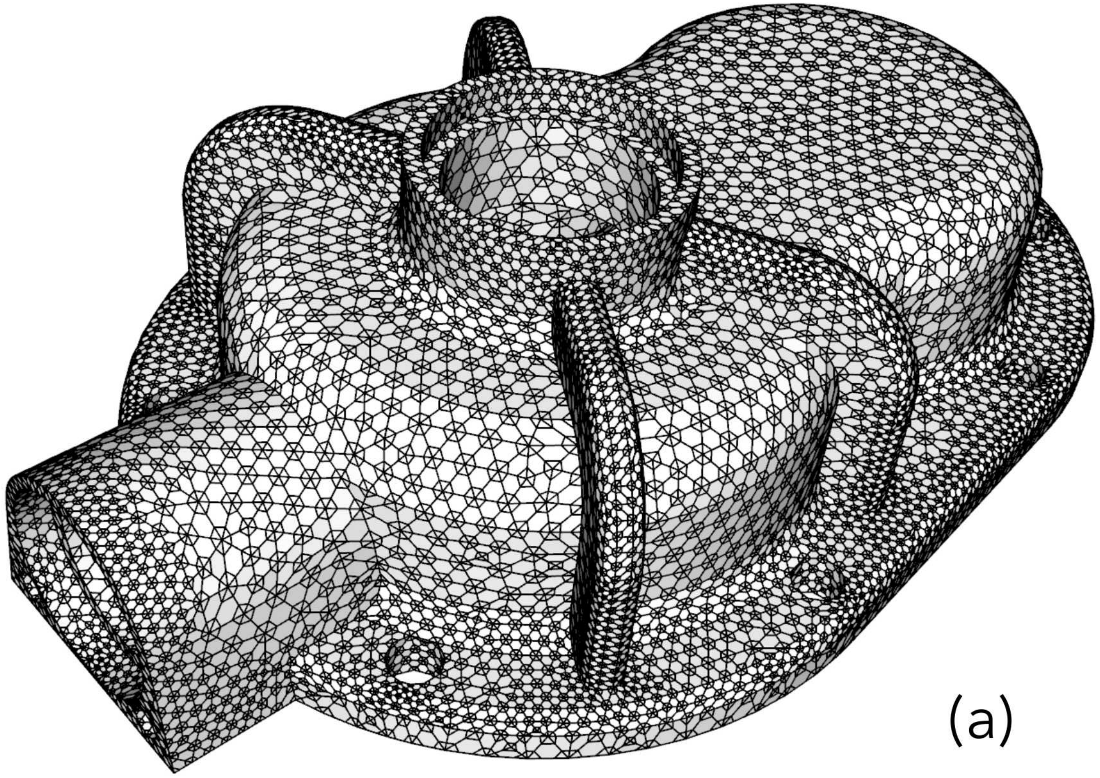

(a)

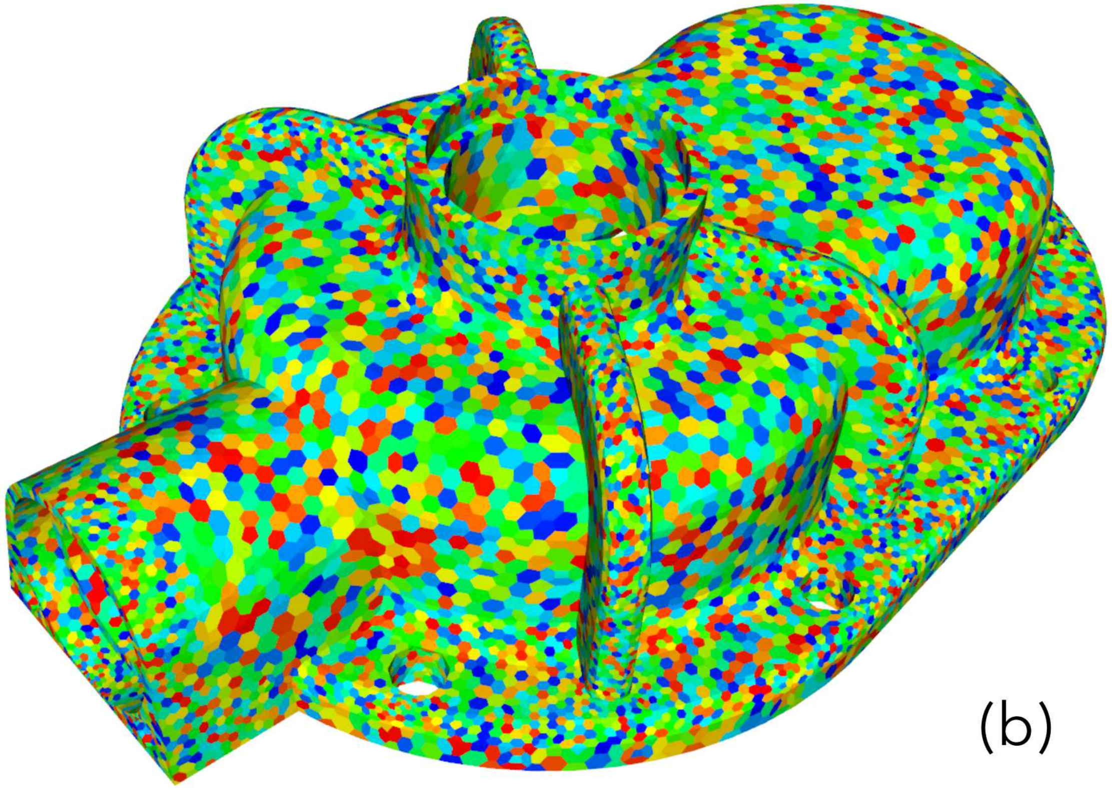

(b)

Element geometry

number of poly element vertices

number of attached tetrahedra

barycentric subdivision

truncated subdivision

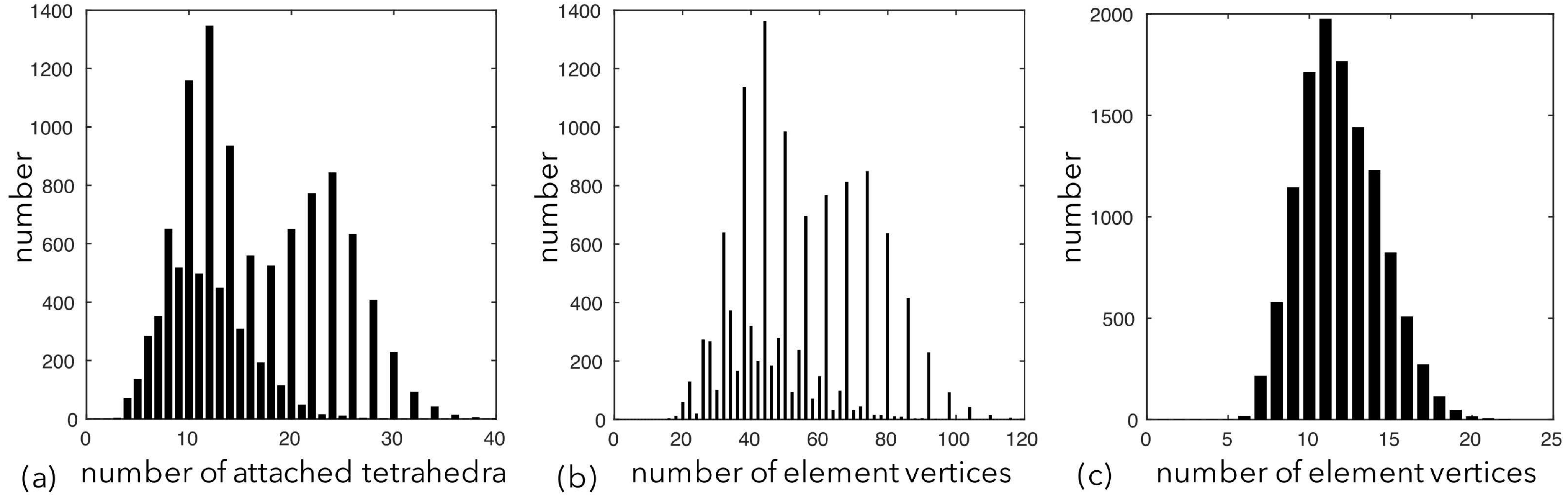

Governing equations (total-Lagrangian formulation)

strong form

$$\frac{\partial \boldsymbol{P}}{\partial \boldsymbol{X}} : \boldsymbol{I} = \rho_0 \, \ddot{\boldsymbol{u}}$$

$$\boldsymbol{u} = \overline{\boldsymbol{u}} \quad \text{on} \quad \Gamma_0^u \quad \text{and} \quad \boldsymbol{P} \cdot \boldsymbol{N} = \boldsymbol{t}_0 \quad \text{on} \quad \Gamma_0^t$$

weak form

find the trial functions $\boldsymbol{u} \in \boldsymbol{H}^1(\Omega_0)$

$$\int_{\Gamma_0^t} \boldsymbol{t}_0 \cdot \boldsymbol{v} \, dS - \int_{\Omega_0} \boldsymbol{P} : (\partial \boldsymbol{v} / \partial \boldsymbol{X}) \, d\boldsymbol{X} = \int_{\Omega_0} \rho_0 \, \ddot{\boldsymbol{u}} \cdot \boldsymbol{v} \, d\boldsymbol{X}$$

for all test functions $\boldsymbol{v} \in \boldsymbol{H}_0^1(\Omega_0)$

Finite element formulation

- Galerkin formulation
- Total-Lagrangian formulation (integrate weak form on original configuration).
- Minimize number of integration points while avoiding artificial stabilization.
- Can use both harmonic and maximum-entropy shape functions .
- Mean-dilation (F-bar) formulation for nearly-incompressible materials
- Compatible with standard trilinear hexahedron

Harmonic shape functions

Harmonic functions minimize the Dirichlet energy given by the following functional:

$$J(\psi) := \frac{1}{2} \int_{\Omega_\mathrm{e}} \nabla\psi \cdot \nabla\psi \, d\boldsymbol{X} \qquad \text{with } \psi \in H^1(\Omega_\mathrm{e})$$

The minimizer of this functional satisfies the following variational problem:

$$\text{find } \psi \in H^1(\Omega_\mathrm{e}) \text{ with } \psi = \overline{\psi} \text{ on } \Gamma_\mathrm{e} \text{ such that}$$

$$\int_{\Omega_\mathrm{e}} \nabla\psi \cdot \nabla v \, d\boldsymbol{X} = 0$$

$$\text{for all test functions } v \in H^1_0(\Omega_\mathrm{e})$$

The strong form of this variational problem is given by:

$$\nabla^2\psi = 0 \text{ in } \Omega_\mathrm{e} \quad \text{with} \quad \psi = \overline{\psi} \text{ on } \Gamma_\mathrm{e}$$

Harmonic shape functions

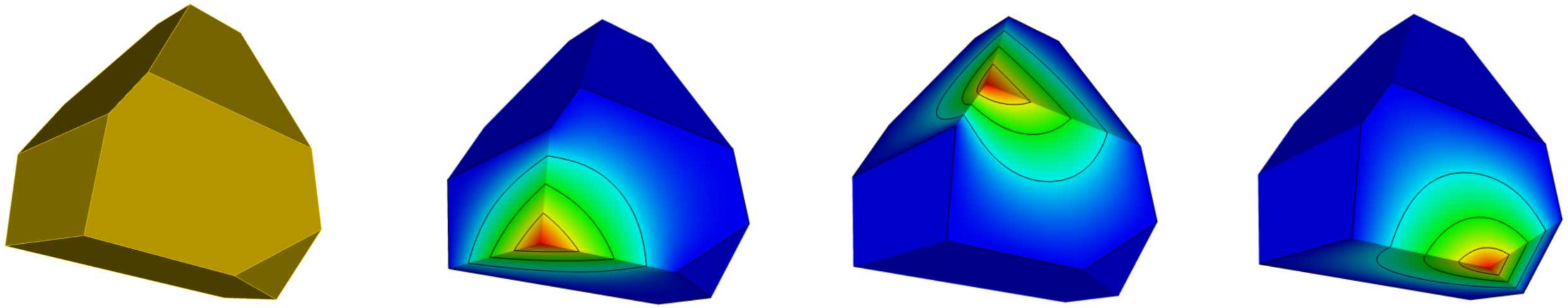

$$\sum_{a=1}^{N_{\mathrm{v}}} \psi_a(\boldsymbol{X}) = 1$$

partition of unity

$$\sum_{a=1}^{N_{\mathrm{v}}} \psi_a(\boldsymbol{X})\, \boldsymbol{X}_a = \boldsymbol{X}$$

linear reproducibility

Maximum-entropy shape functions

For a given $\boldsymbol{X} \in \Omega_{\mathrm{e}}$, the shape functions $\psi_a(\boldsymbol{X}), a = 1, \ldots, N_{\mathrm{v}}$, are found by minimizing the functional

$$J(\psi_a, a = 1, \ldots N_{\mathrm{v}}) := \sum_{a=1}^{N_{\mathrm{v}}} \psi_a(\boldsymbol{X}) \ln \left(\frac{\psi_a(\boldsymbol{X})}{w_a(\boldsymbol{X})} \right)$$

$w_a(\boldsymbol{X})$ is a suitable *prior* weight function

subject to the reproducing constraints $\displaystyle\sum_{a=1}^{N_{\mathrm{v}}} \psi_a(\boldsymbol{X}) = 1 \quad \sum_{a=1}^{N_{\mathrm{v}}} \psi_a(\boldsymbol{X})\, \boldsymbol{X}_a = \boldsymbol{X}$

This constrained optimization problem can be solved using the method of Lagrange multipliers:

$$\mathcal{L}(\psi_a, \lambda_0, \boldsymbol{\lambda}) := \sum_{a=1}^{N_{\mathrm{v}}} \psi_a(\boldsymbol{X}) \ln \left(\frac{\psi_a(\boldsymbol{X})}{w_a(\boldsymbol{X})} \right) + \lambda_0 \left(\sum_{a=1}^{N_{\mathrm{v}}} \psi_a(\boldsymbol{X}) - 1 \right) + \boldsymbol{\lambda} \cdot \left(\sum_{a=1}^{N_{\mathrm{v}}} \psi_a(\boldsymbol{X})\, \boldsymbol{X}_a - \boldsymbol{X} \right)$$

Comparison

(Hormann, K. and N. Sukumar, 2008)

harmonic max-ent

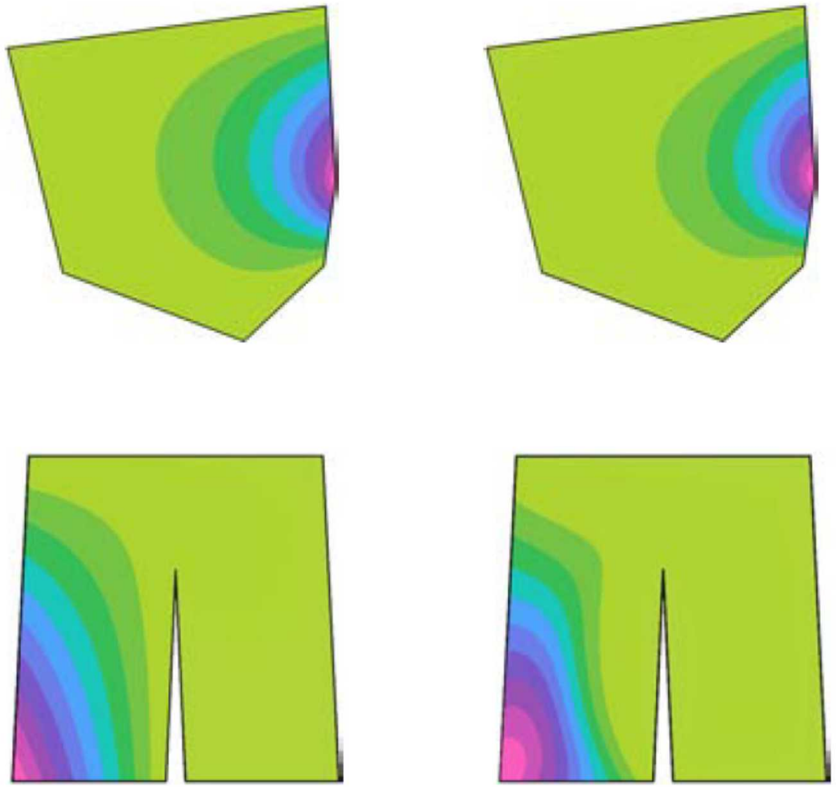

Element integration

- Due to computational expense of plasticity models, want to minimize the number of quadrature points.
- Follow approach of Rashid and Selimotec, 2006.
- Each node is associated with a "tributary" volume.
- Number of quadrature points is equal to the number of vertices.
- Quadrature weight = volume of tributary volume.
- First-order accurate, but quadrature weights are positive (avoids Runge's phenomenon)

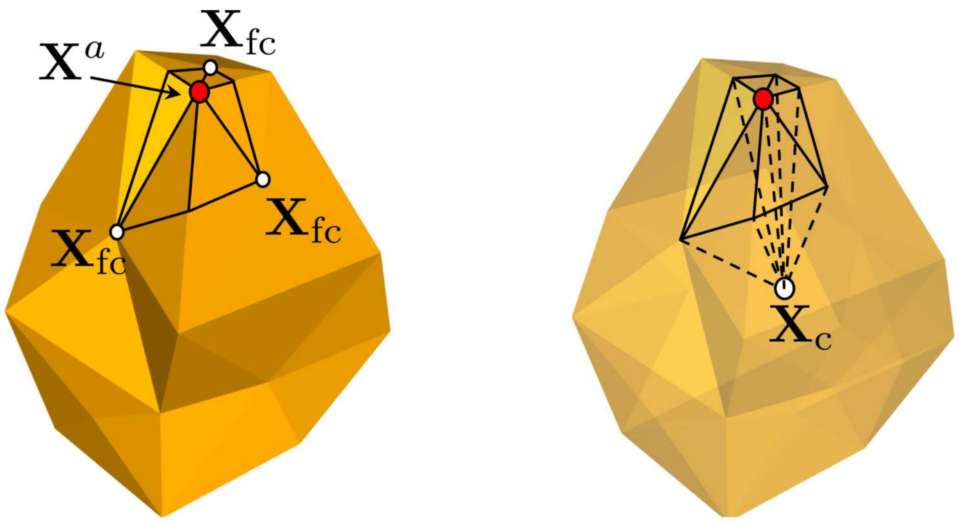

Integration consistency

Divergence theorem states that:

$$\int_{\Omega_\mathrm{e}} \nabla\psi_a \, d\boldsymbol{X} = \int_{\Gamma_\mathrm{e}} \psi^a \, \boldsymbol{N} \, dS$$

where $\boldsymbol{N}$ is the outward unit normal vector on Γ_e

In discrete form:

$$\sum_{k=1}^{N_\mathrm{Q}} w_k \nabla\psi_{ak} = \sum_{l=1}^{N_\mathrm{Q}^\Gamma} w_l^\Gamma \, \psi_{al} \, \boldsymbol{N}_l \ , \quad (a = 1, \ldots, N_\mathrm{v})$$

where $\psi_{ak} := \psi_a(\boldsymbol{X}_k)$, and $\boldsymbol{X}_k$ is the position of the k-th quadrature point

- For non-polynomial shape functions, this will not be satisfied in general.
- This will results in a lack of consistency (failure of the engineering patch test).

Shape function derivative correction

- "Tweak" the shape function derivatives to satisfy the integration consistency condition.
- Maintain the reproducing properties of the derivatives.
- Minimize the least-squares difference between the new derivatives and the old.

$$\min_{\boldsymbol{\xi}_k \in \boldsymbol{R}^3} \sum_{k=1}^{N_\mathrm{Q}} w_k ||\boldsymbol{\xi}_k - \nabla\psi_{ak}||^2 \qquad \text{subject to the constraints} \qquad \sum_{k=1}^{N_\mathrm{Q}} w_k\, \boldsymbol{\xi}_k - \sum_{l=1}^{N_\mathrm{Q}^\Gamma} w_l^\Gamma \psi_{al} \boldsymbol{N}_l = 0$$

This constrained optimization problem can be solved using the method of Lagrange multipliers:

$$\mathcal{L}(\boldsymbol{\xi}_k, \boldsymbol{\lambda}) := \sum_{k=1}^{N_\mathrm{Q}} w_k ||\boldsymbol{\xi}_k - \nabla\psi_{ak}||^2 + \boldsymbol{\lambda} \cdot \left(\sum_{k=1}^{N_\mathrm{Q}} w_k\, \boldsymbol{\xi}_k - \sum_{l=1}^{N_\mathrm{Q}^\Gamma} w_l^\Gamma \psi_{al} \boldsymbol{N}_l \right)$$

Patch test

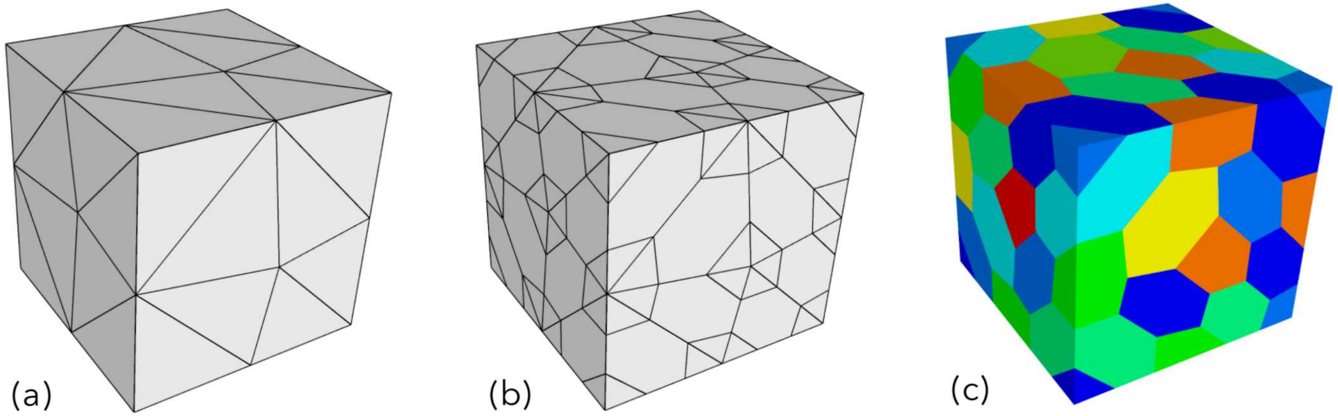

tension

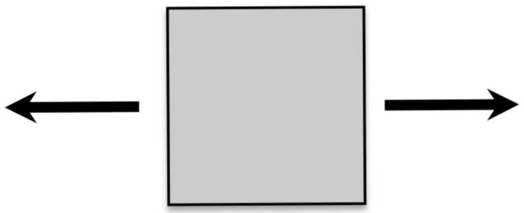

shear

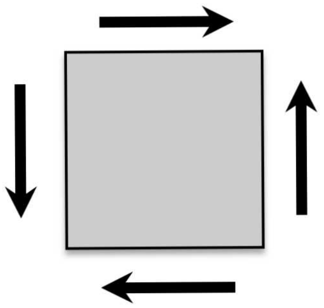

Patch test

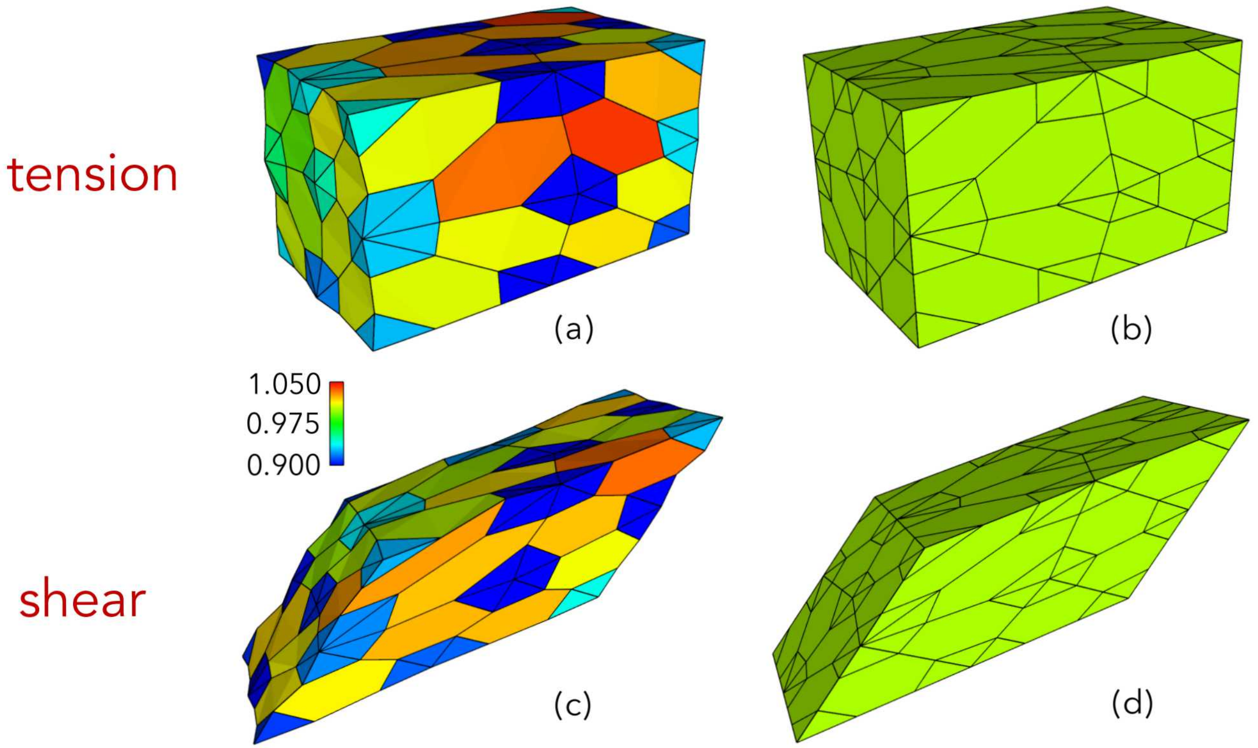

Error in stress with and without correction

applied traction state	without correction	with correction
tension	0.18	$9.6 \cdot 10^{-13}$
shear	0.13	$2.7 \cdot 10^{-12}$

examples

Beam bending with shear load

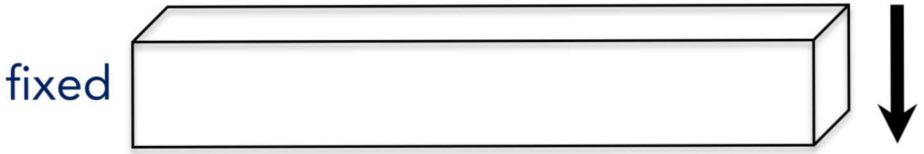

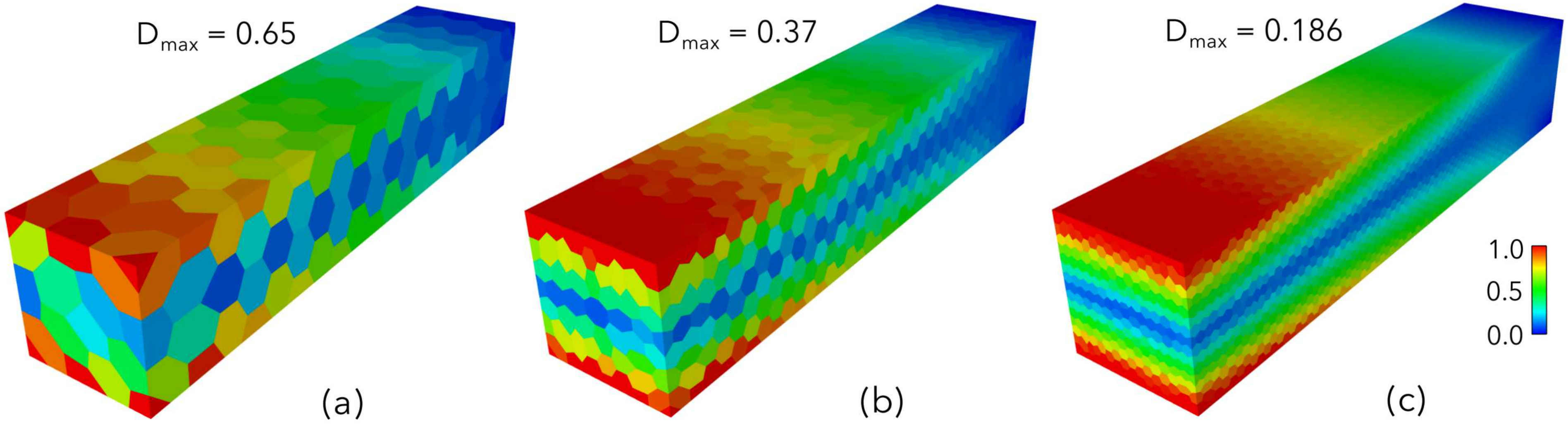

Convergence, harmonic vs. max-ent

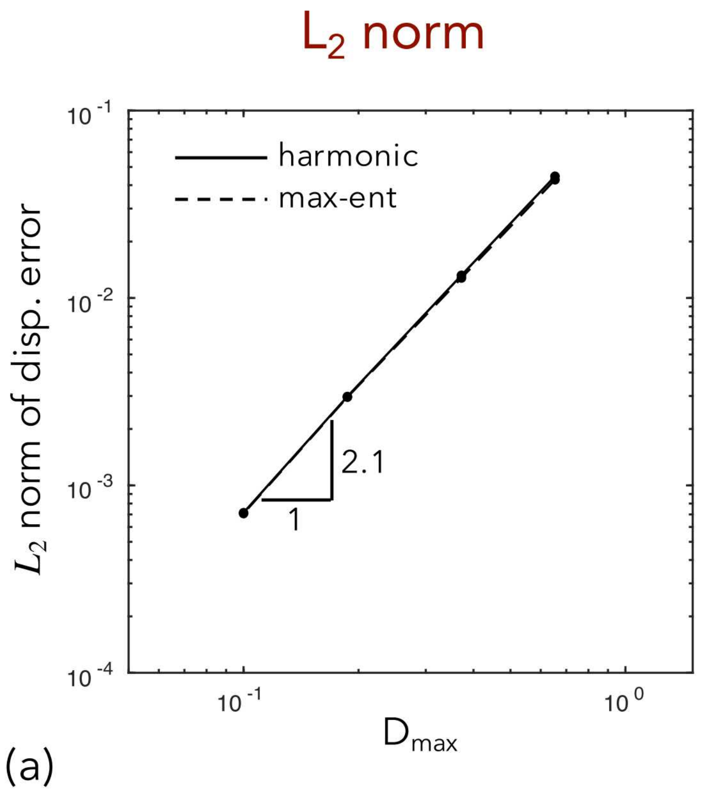

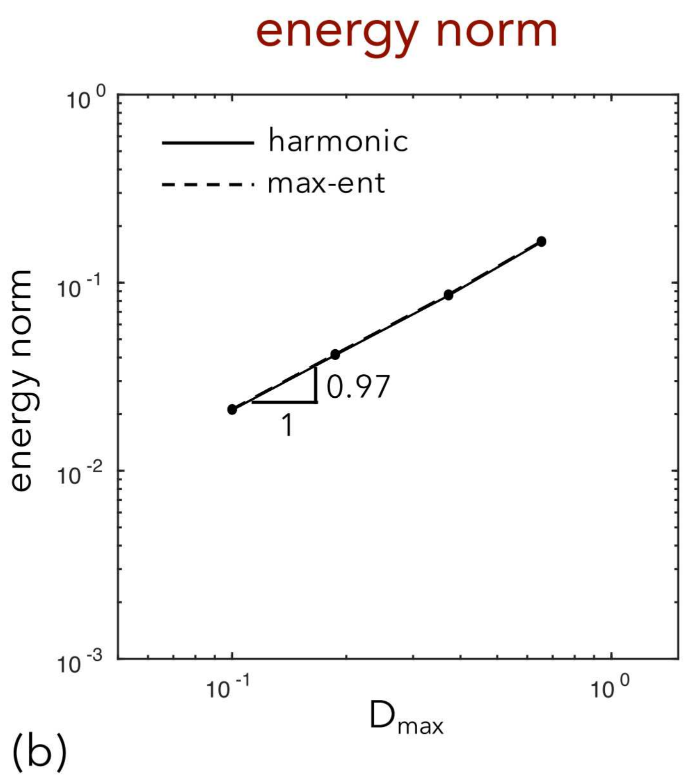

Convergence, harmonic vs. max-ent

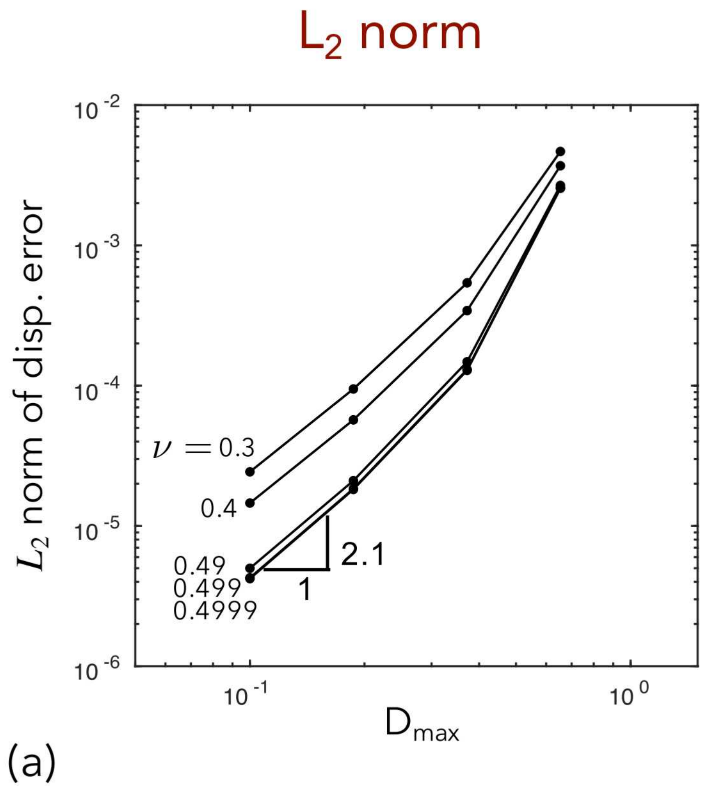

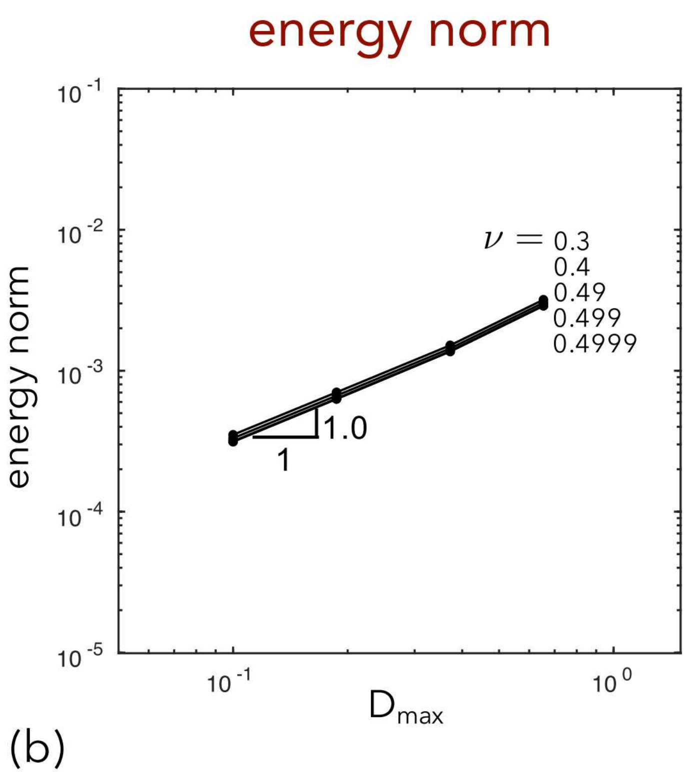

Example: large-deformation torsion

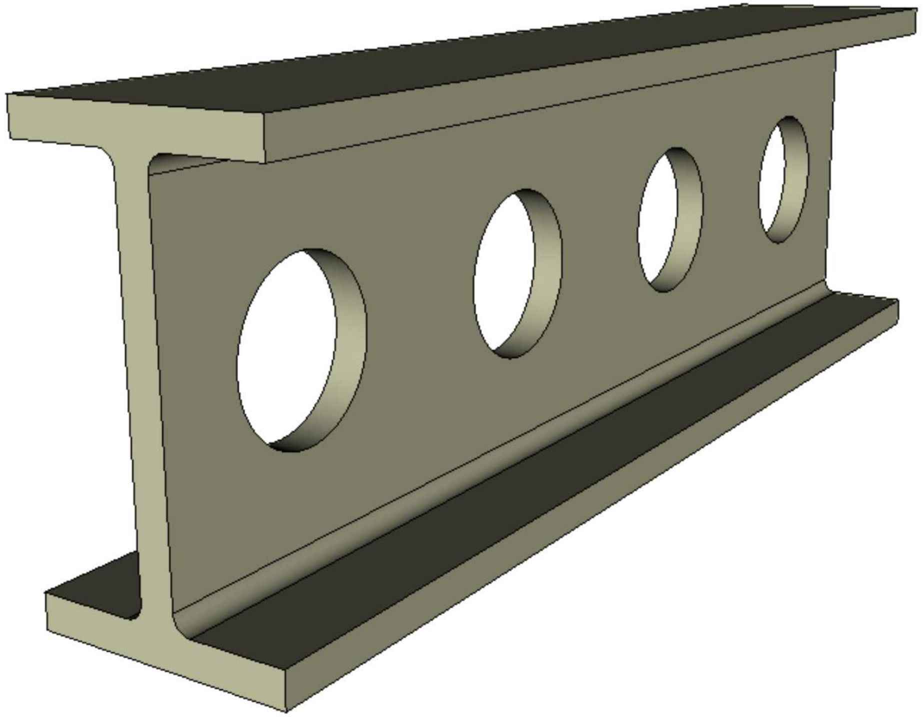

- torsion loading, 90° rotation
- neo-Hookean hyperelastic

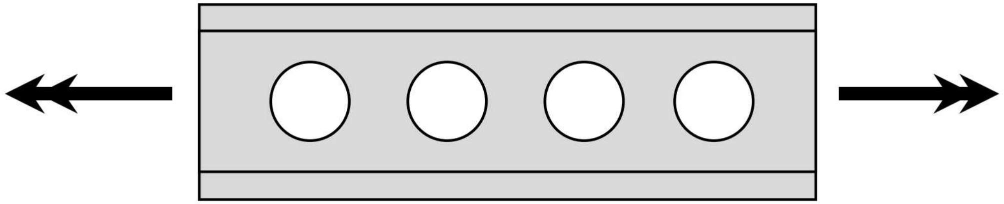

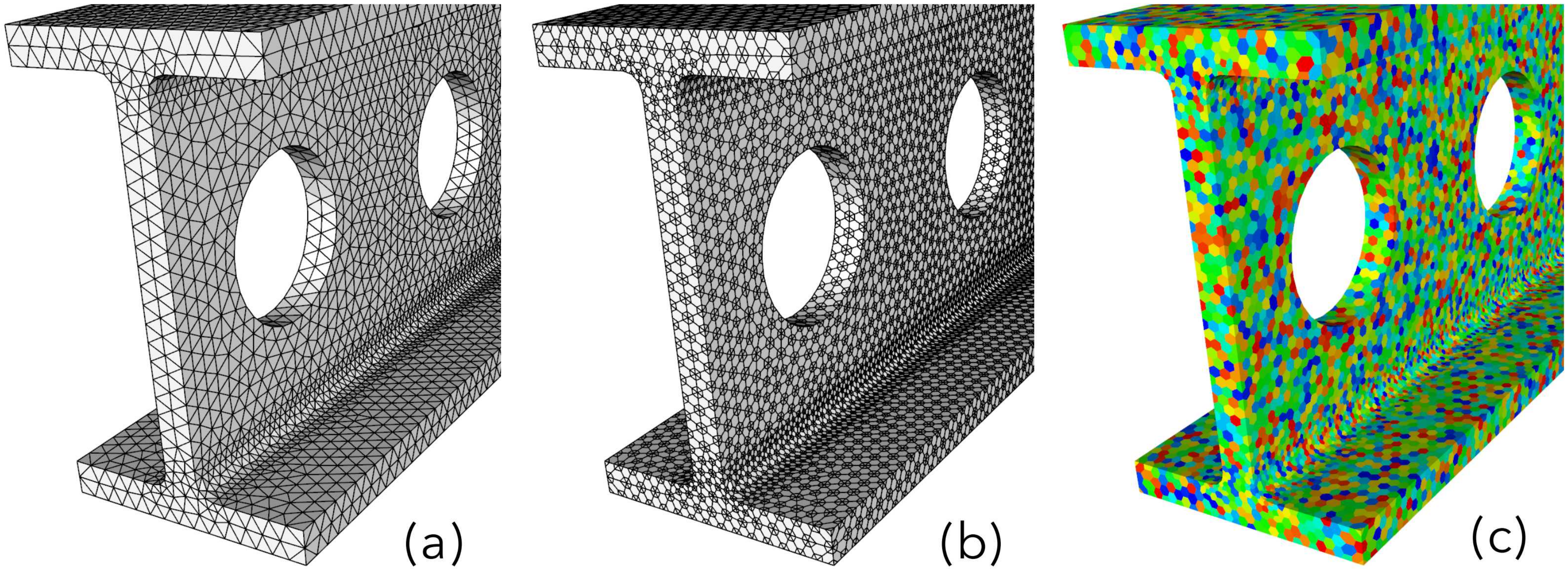
(a)
(b)
(c)

polyhedral mesh

conventional hexahedral mesh

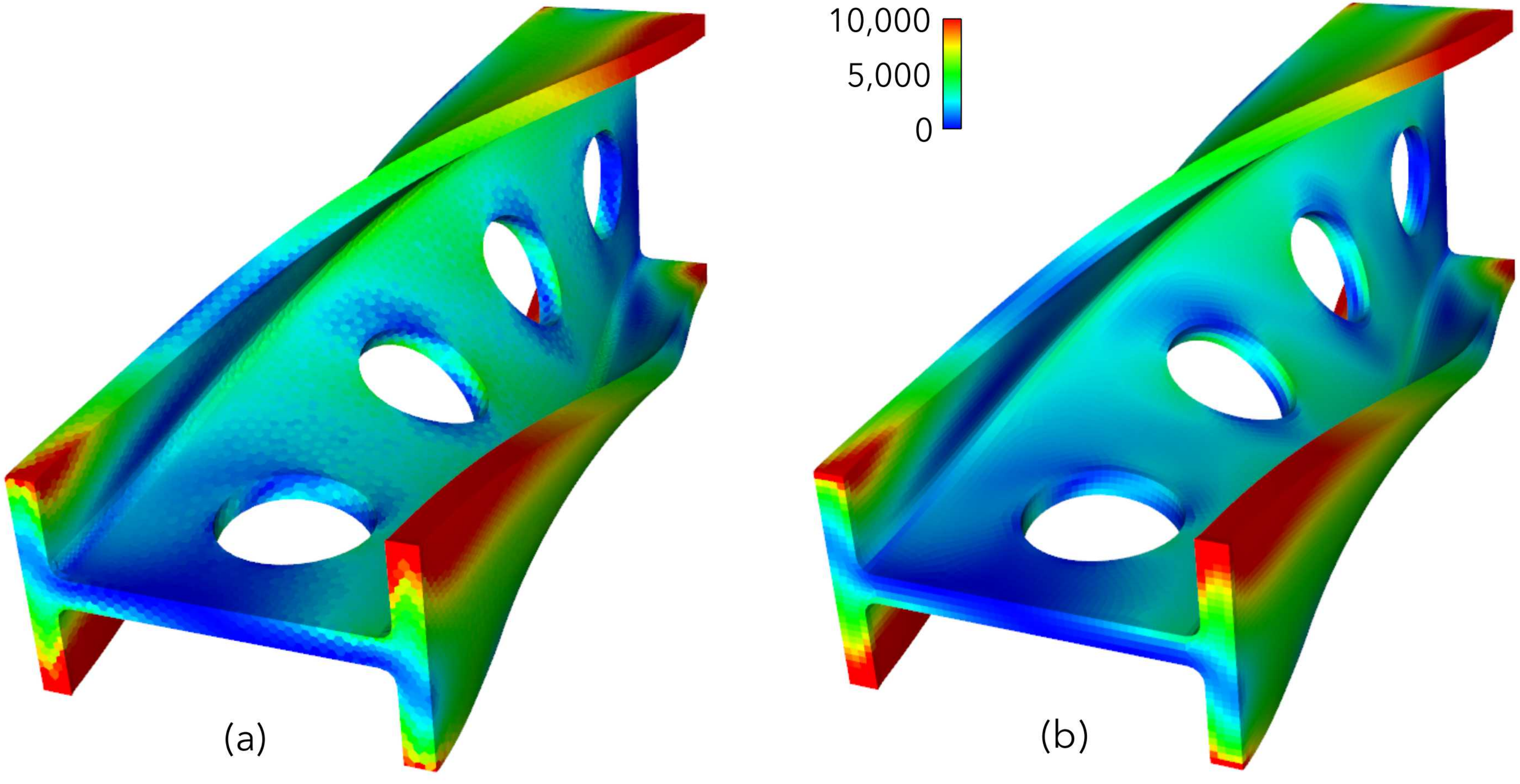

von Mises stress field

Comparison of reaction forces

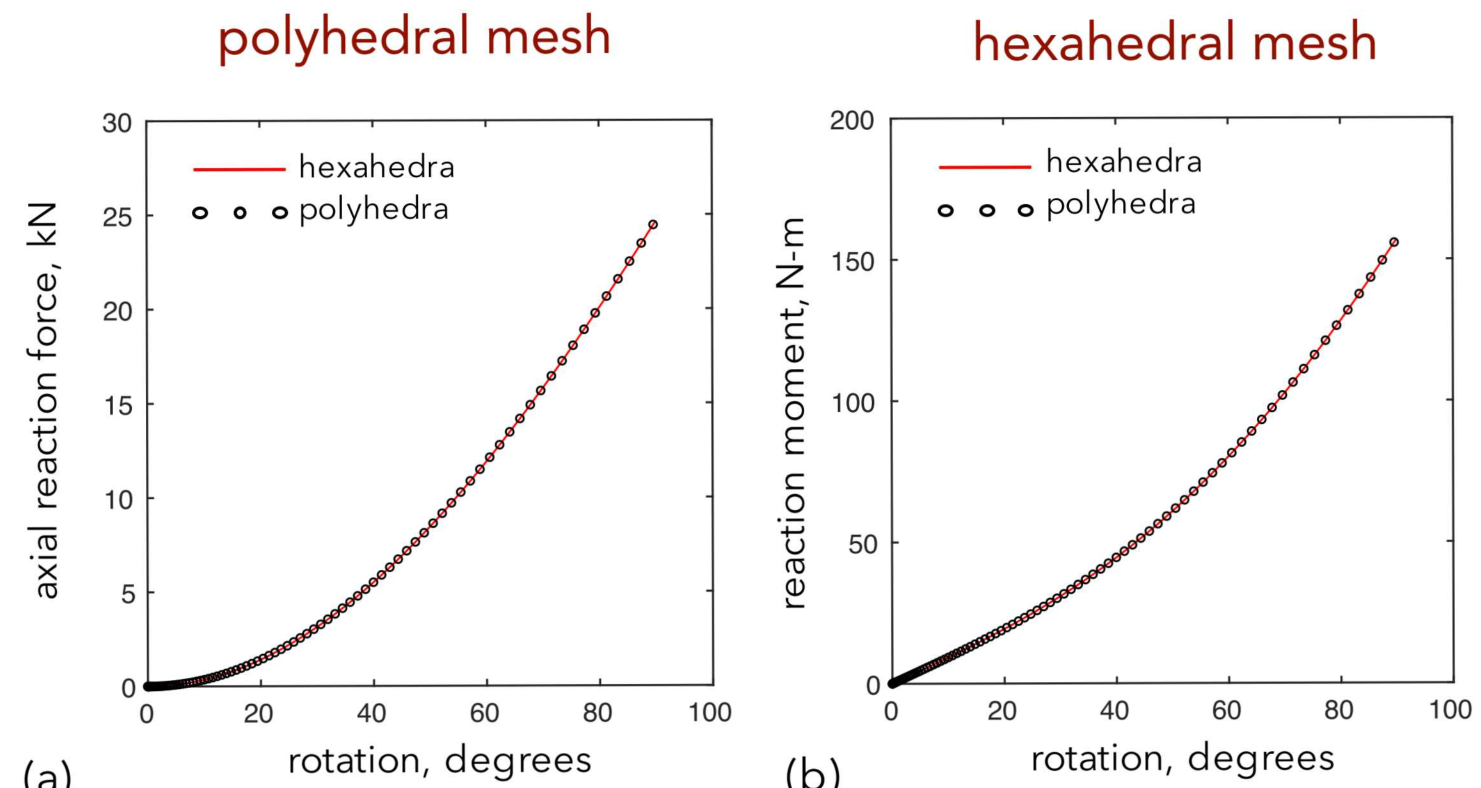

(a) (b)

Example: elastic-plastic plate

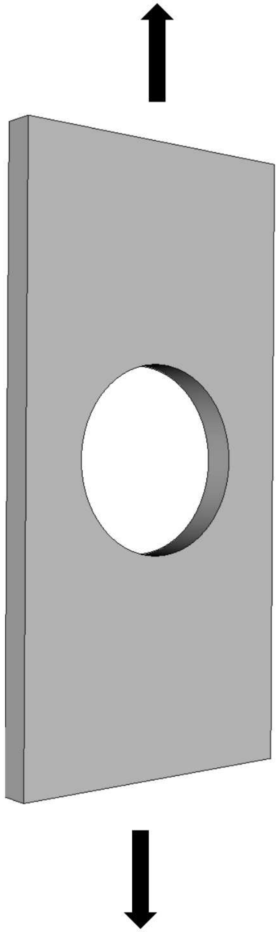

- uniaxial extension
- elastic-plastic constitutive model

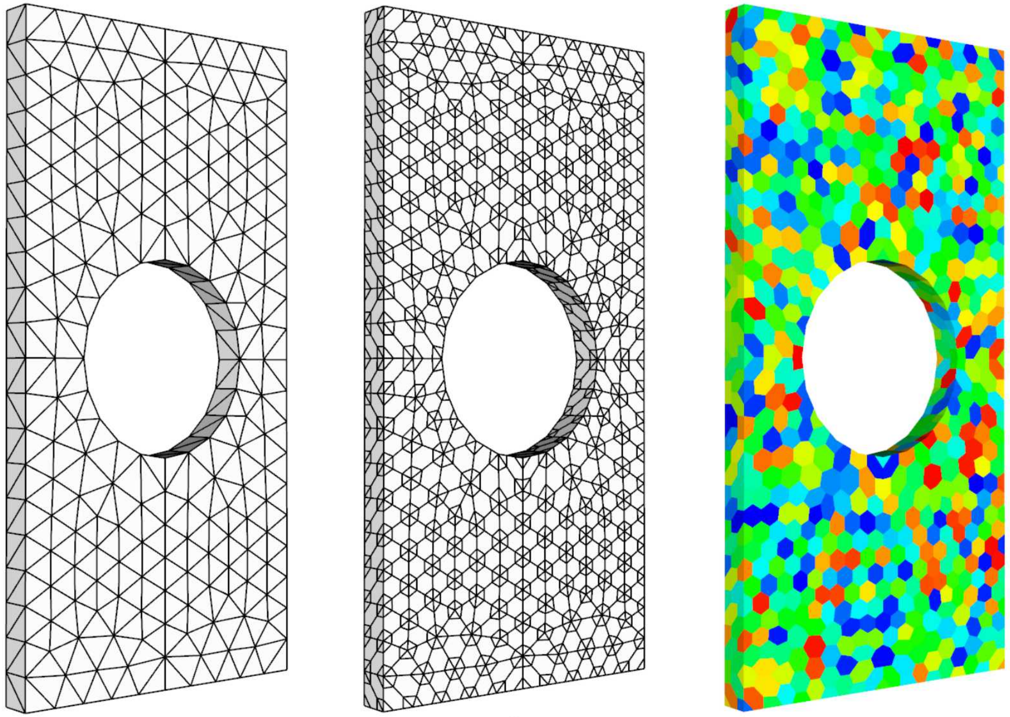

Simulation results

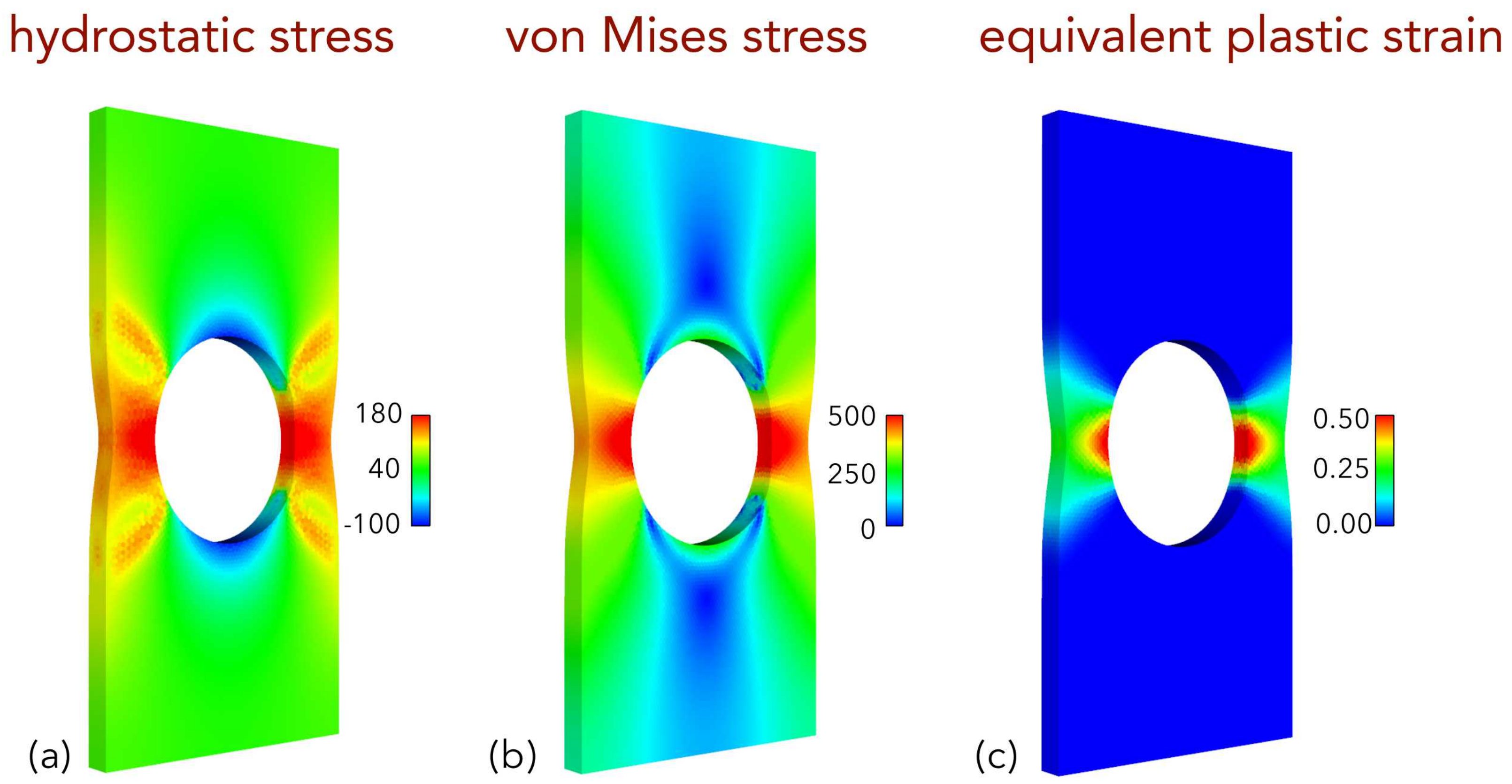

Comparison of reaction forces

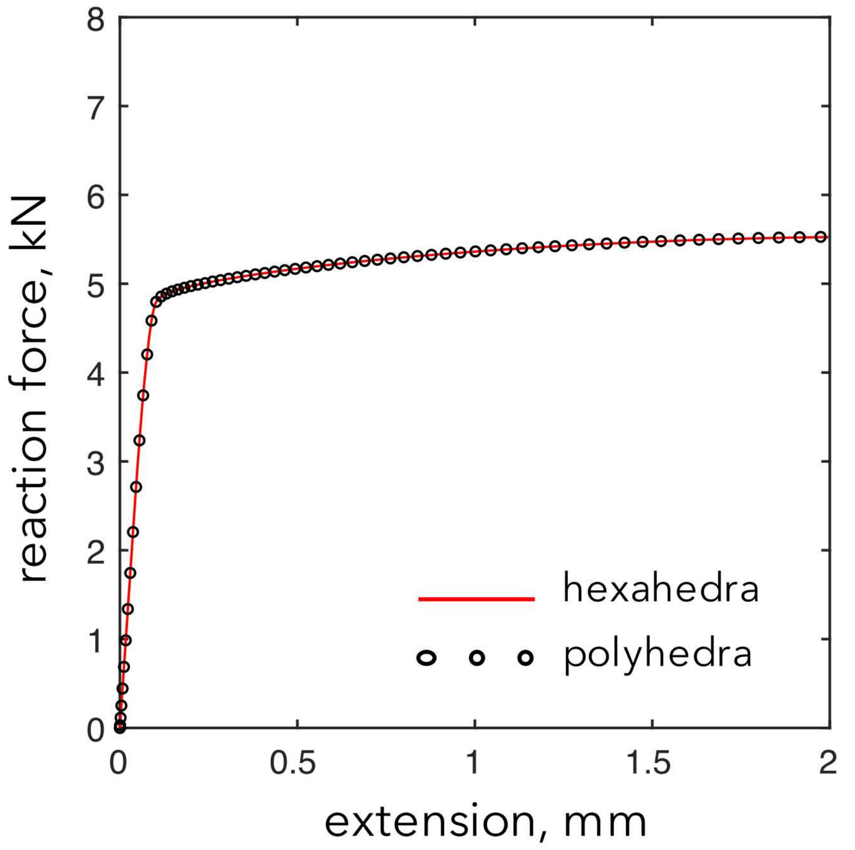

Final example

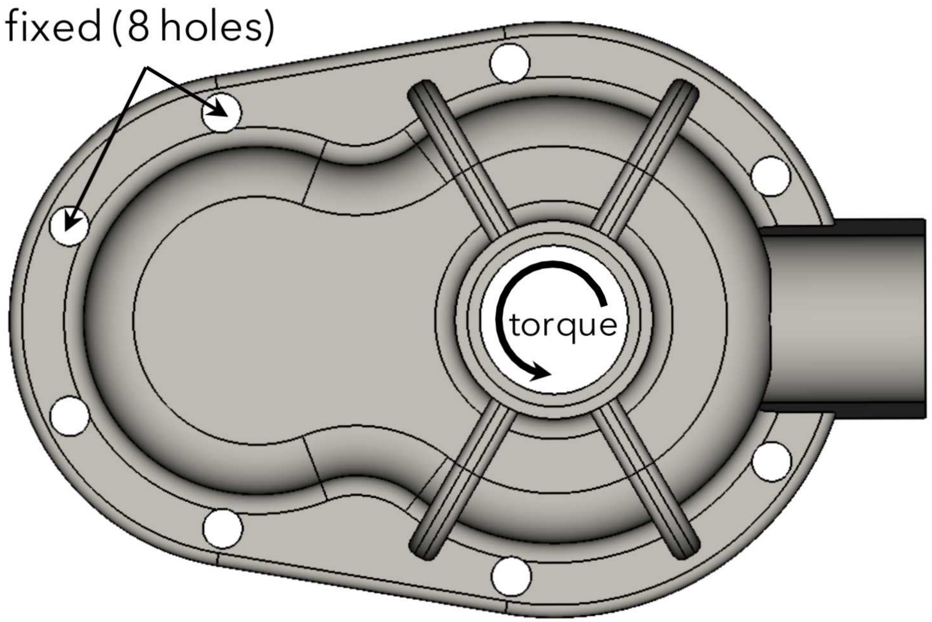

von Mises stress field

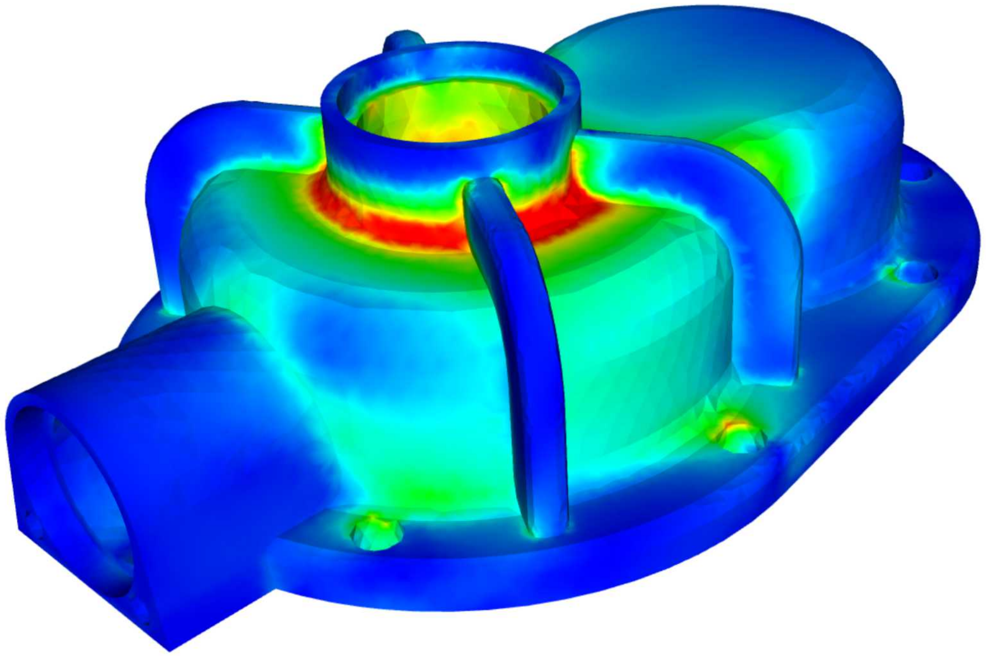

Similar results using either Max-ent or harmonic.

Summary

1. Demonstrated a class of polyhedral discretizations on complex shapes through tetrahedral subdivision and aggregation.
2. Can use both harmonic and MAXENT.
3. Need further development to optimize integration on 12-vertex ochahedron. Could also use Wachpress on this element.
4. Need to compare with tetrahedral elements for nonlinear solid mechanics.

References

- Bishop, J. and Sukumar, N., "Polyhedral finite elements for nonlinear solid mechanics using tetrahedral subdivisions and dual-cell aggregation," *Computer Aided Geometric Design*, (submitted)
- Bishop, J., "A displacement-based finite element formulation for general polyhedra using harmonic shape functions," *Int. J. for Numerical Methods in Engineering*, 2014, 97:1-31.
- Bishop, J., "Simulating the pervasive fracture of materials and structures using randomly close packed Voronoi tessellations," *Computational Mechanics*, 2009, 44:455-471.